S. Vijayalakshmi[1]
R. Balaji Rao[1]
I. L. Karle[2]
P. Balaram[3]

[1] *Department of Chemistry, Banaras Hindu University, Varanasi-221005, India*

[2] *Laboratory for the Structure of Matter, Naval Research Laboratory, Washington, DC, 20375-5341, USA*

[3] *Molecular Biophysics Unit, Indian Institute of Science, Bangalore-560012, India*

Received 7 May 1998; accepted 21 May 1999

Comparison of Helix-Stabilizing Effects of α,α-Dialkyl Glycines with Linear and Cycloalkyl Side Chains

Abstract: *The ability of α,α-di-n-alkyl glycines with linear and cyclic alkyl side chains to stabilize helical conformations has been compared using a model heptapeptide sequence. The conformations of five synthetic heptapeptides (Boc–Val–Ala–Leu–Xxx–Val–Ala–Leu–OMe, Xxx = Ac_8c, Ac_7c, Aib, Dpg ,and Deg, where Ac_8c = 1-aminocyclooctane-1-carboxylic acid, Ac_7c = 1-aminocycloheptane-1-carboxylic acid, Aib = α-aminoisobutyric acid, Dpg = α,α-di-n-propyl glycine, Deg = α,α-di-n-ethyl glycine) have been investigated. In crystals, helical conformations have been demonstrated by x-ray crystallography for the peptides, R–Val–Ala–Leu–Dpg–Val–Ala–Leu–OMe, (R = Boc and acetyl). Solution conformations of the five peptides have been studied by ^{1}H-nmr. In the apolar solvent $CDCl_3$, all five peptides favor helical conformations in which the NH groups of residues 3–7 are shielded from the solvent. Successive $N_iH \leftrightarrow N_{i+1}H$ nuclear Overhauser effects over the length of the sequence support a major population of continuous helical conformations. Solvent titration experiments in mixtures of $CDCl_3$/DMSO provide evidence for solvent-dependent conformational transitions that are more pronounced for the Deg and Dpg peptides. Solvent-dependent chemical shift variations and temperature coefficients in DMSO suggest that the conformational distributions in the Deg/Dpg peptides are distinctly different from the Aib/Ac_nc peptides in a strongly solvating medium. Nuclear Overhauser effects provide additional evidence for the population of extended backbone conformations in the Dpg peptide, while a significant residual population of helical conformations is still detectable in the isomeric Ac_7c peptide in DMSO.* © 2000 John Wiley & Sons, Inc. Biopoly 53: 84–98, 2000

Keywords: *heptapeptides; alpha-helix; 3_{10}-helix; crystal structures; solution structures; helix transitions; solvent dependency*

Correspondence to: P. Balaram; email: pb@mbu.iisc.ernet.in

Contract grant sponsor: Department of Science & Technology, Government of India, the National Institute of Health (NIH), and the Office of Naval Research

Contract grant number: GM-30902 (NIH)

Biopolymers, Vol. 53, 84–98 (2000)

CCC 0006-3525/00/010084-15

INTRODUCTION

The introduction of a second alkyl group at the α-carbon atom results in a dramatic restriction in the range of accessible backbone conformations for α, α-di-n-alkylglycines as compared to the standard protein amino acids.[1,2] α-Aminoisobutyric acid (Aib), a constituent of several membrane-active natural peptides,[3–5] is the most extensively investigated member of the family of α, α-dialkylated residues and has been shown to be an extremely strong stabilizer of helical conformations in oligopeptides.[2,6–12] Oligopeptides (≥7 residues) of nonpolar L-amino acids (Ala, Leu, Val, Ileu, Phe, Met) are generally poorly soluble in organic solvents and have a great tendency to form self-associated structures. Incorporation of even a single Aib residue promotes intramolecular helix formation resulting in highly soluble peptides that dissolve in a variety of nonpolar solvents.[13–15] Helix formation in apolar peptides of length 6–9 residues can be achieved by placement of a single Aib residue at a central position with several examples being characterized in crystals.[7] A model heptapeptide, Boc–Val–Ala–Leu–Aib–Val–Ala–Leu–OMe, has been used in our laboratory as a preformed helical module in the assembly of synthetic helix–helix motifs.[16,17] Crystal structure determinations of this heptapeptide in different polymorphic forms have revealed evidence for solvated helical backbones and partially unfolded termini, suggesting that this sequence is delicately poised with respect to unfolding as a function of environmental conditions.[18,19] The potential fragility of this designed helix may be used to advantage in probing the relative helix-stabilizing abilities of diverse α, α-dialkyl amino acids. Conformational energy calculations suggest that helical regions of ϕ,ψ-space are a pronounced energy minima in the case of Aib[1,2] and 1-aminocycloalkane-1-carboxylic acids (Ac_nc),[20] whereas in the case of dialkylglycines with linear alkyl chains (Dxg), fully extended structures appear to be marginally lower in energy than helical conformations.[21] The preferred conformations reported for the Ac_nc residues parallel those of the prototype residue Aib.[22–25] Nuclear magnetic resonance studies showed that tripeptides containing Dxg residues promote extended conformation in solution, whereas the Ac_nc residues promote folded conformation in analogous sequences under identical conditions.[26] In the case of dipropylglycine (Dpg), both extended[27–29] and helical conformations[30–32] have been characterized in peptide crystal structures. Experimental results on Deg-containing peptides suggest that these residues favor fully extended conformation in homooligopeptides.[33] In principle, therefore, helices formed with Dxg peptides may be more susceptible to unfolding as compared to Aib- and Ac_nc-containing structures. We have chosen to examine a series of heptapeptides, Boc–Val–Ala–Leu–Xxx–Val–Ala–Leu–OMe (Xxx = Ac_8c, Ac_7c, Aib, Dpg, and Deg) in an apolar solvent $CDCl_3$, where helices are expected to be favored, and in a polar-solvating medium $(CD_3)_2SO$, where unfolded solvated structures can be populated.[34] The results demonstrate that the Deg and Dpg peptides have a significantly greater tendency to unfold in a strongly interacting solvent. Helical conformations are demonstrated for two variants of the Dpg heptapeptide in single crystals by x-ray diffraction.

EXPERIMENTAL PROCEDURES

Synthesis of Amino Acids and Peptides

$C^{\alpha,\alpha}$-dialkylated amino acids were synthesized from the appropriate ketones in good yield and purity by reported procedures.[27,35]

The peptides were synthesized by conventional solution phase procedures using a fragment condensation strategy. For the Aib and Ac_nc peptides, fragment couplings could be achieved in high yield when the Aib/Ac_nc residues were at the C-terminus. For the Dxg peptides the unit Leu–Dxg–Val was extended in both N- and C-terminal directions to overcome the problem of low coupling yields in fragment condensation when Dxg was at the C-terminus. The Boc group was used for the N-terminal protection and the C-terminus was protected as a methyl ester. Deprotections were performed using 98% formic acid or saponification, respectively. Coupling reactions in the preparation of dipeptides were mediated by dicyclohexylcarbodiimide (DCC) in dichloromethane (DCM) and all other couplings were carried out in dimethylformamide (DMF), in the presence of DCC and 1-hydroxybenzotriazole (HOBt). All the intermediate peptides were characterized by ^{1}H-nmr (80 MHz) and thin layer chromatography (TLC), and used without further purification. The final peptides were purified by medium pressure liquid chromatography on a reversed phase C_{18} column. Homogeneity was established by high performance liquid chromatography (HPLC) on a (4 × 250 mm particle size 5 μ) C_{18} column using methanol/water gradients. All final peptides were fully characterized by 500 MHz ^{1}H-nmr and FAB mass spectrometry. Representative synthetic procedures for the peptides in the Ac_nc and Dxg series are given below. Physical characteristics and mass spectral characteristics for all the peptides are summarized in Table I.

Synthesis of Boc–Val–Ala–Leu–Ac_8c–Val–Ala–Leu–OMe (Ac_8c-7)

Boc–Leu–Ac_8c–OMe (1). Boc–Leu–OH (2.30g, 10 mmol) was dissolved in dichloromethane (7 mL) and cooled in an ice bath. H_2N–Ac_8c–OMe isolated from 3.5 g (16.5

Table I Physical Characteristics of the Peptides Boc–Val–Ala–Leu–Xxx–Val–Ala–Leu–OMe

Xxx ↓	HPLC[a] Retention Time (in minutes)	mp[b] (in °C)	M_{calcd} (Da)	M_{obs} [c] $[M + Na]^+$ (Da)
Ac_8c	27.5	223.8	850	873
Ac_7c	25.4	210.9	836	859
Aib	15.1	194.8	783	807[d]
Dpg	25.0	196.7	838	861
Deg	20.4	201.5	810	833

[a] Solvent gradient 60–95% methanol in 50 min. Column: RP. C_{18} (4 × 250 mm particle size 5 μ). Flow: 0.8 mL/min.

[b] Melting points are uncorrected.

[c] Molecular ion masses in fast atom bombardment mass spectra.

[d] $[M + Na]^+$ determined by matrix-assisted laser desorption/ionization time of flight mass spectra. MH^+ determined by electrospray ionization is 784.

mmol) of its hydrochloride was added, followed by DCC (2.06g, 10 mmol) and stirred for 36 h at room temperature. Dichloromethane was evaporated, the residue was diluted with ethylacetate, and DCU filtered. The solution was washed with 2N HCl (3 × 50 mL), brine (3 × 50 mL), 1*M* Na_2CO_3 (3 × 50 mL) and water (50 mL). The organic layer after drying over anhydrous Na_2SO_4 and evaporation under reduced pressure afforded 3.9 g (98%) of a white solid. ^{1}H-nmr (80 MHz,$CDCl_3$, δ): 0.90, 6H (Leu $C^{\delta}H_3$); 1.40, 9H, s (Boc CH_3); 1.50, 1.63 17H (Ac_8c ring protons, Leu $C^{\beta}H_2/C^{\gamma}H$); 3.65, 3H, s (—O—CH_3); 3.95, 1H, m (Leu $C^{\alpha}H$); 4.85, 1H, d (Leu NH); 6.38, 1H, s (Ac_8c NH).

Boc–Leu–Ac_8c–OH (2). Boc–Leu–Ac_8c–OMe (3.58g, 9 mmol) was dissolved in methanol (9 mL) and 4N NaOH (4 mL) was added. The reaction mixture was stirred at room temperature, and the progress of the reaction monitored by TLC. After completion of the reaction, methanol was evaporated, and the residue taken in water and washed with ether. The aqueous layer was cooled in an ice bath, and acidified to pH 2 with 6N HCl and extracted with ethylacetate (3 × 50 mL). The organic layer after drying over anhydrous Na_2SO_4 and evaporation under reduced pressure afforded 3.26 g (8.54 mmol, 95%) of a white solid.

Boc–Leu–Ac_8c–Val–Ala–Leu–OMe (3): Boc–Leu–Ac_8c–OH, 2.104 g (6 mmol) was coupled to 2.2 g (7 mmol) of H_2N–Val–Ala–Leu–OMe[31] using DCC (1.648 g, 8 mmol) and HOBt (810 mg, 6 mmol) in DMF, with stirring for 5 days at room temperature. The mixture was diluted with ethylacetate and the DCU filtered. The filtrate was washed with brine (50 mL), 2N HCl (3 × 50 mL), brine (50 mL), 1M Na_2CO_3 (3 × 50 mL) and again with brine (50 mL). The organic layer was dried over anhydrous Na_2SO_4 and evaporated under reduced pressure to afford 3.27 g (4.8 mmol, 80%) of the pentapeptide as a white solid. ^{1}H-nmr (80 MHz, $CDCl_3$, δ): 0.90, 18H (Leu $C^{\delta}H_3$, Val $C^{\gamma}H_3$); 1.40, 1.47, 1.63, 24 H (Ala $C^{\beta}H_3$, Ac_8c ring protons, Leu $C^{\beta}H_2$, $C^{\gamma}H$, Val $C^{\beta}H$); 1.50, 9H, s (Boc CH_3); 3.65, 3H, s (—O—CH_3); 3.95—4.35, 4H, m (Val/Ala/Leu $C^{\alpha}H$) 4.85, 1H, d (Leu NH); 6.60, 1H, s (Ac_8c NH); 6.6–7.6, 3H (Val/Ala/Leu NH)

H_2N–Leu–Ac_8c–Val–Ala–Leu–OMe (4). Deprotection of ***3*** (2.7 g, 4 mmol) was done using 18 mL of 98% formic acid for 16 h at room temperature. After completion of the reaction, excess formic acid was evaporated, the residue taken in water, and washed with ether (2 × 15 mL). The pH of the aqueous layer was adjusted to 8 with Na_2CO_3. The product was extracted into ethylacetate (3 ×50 mL). The ethylacetate layer was dried over anhydrous Na_2SO_4 evaporated under reduced pressure to afford 1.58 g (2.72 mmol, 68%) of the free amine as a gum, which was ninhydrin positive.

Boc–Val–Ala–Leu–Ac_8c–Val–Ala–Leu–OMe (5). Boc–Val–Ala–OH (0.518 g, 1.8 mmol) was coupled to 1.58 g (2.7 mmol) of ***4*** using DCC (0.515 g, 2.5 mmol) and HOBt (0.24 g, 1.8 mmol) in DMF by stirring for 6 days at room temperature. The mixture was diluted with ethylacetate and DCU filtered. The filtrate was washed with brine (50 mL), 2N HCl (3 × 50 mL), brine (50 mL), 1*M* Na_2CO_3 (3 × 5 0 mL) and again with brine (50 mL). The organic layer was dried over anhydrous Na_2SO_4 and evaporated under reduced pressure to afford 1.45 g (1.71 mmol, 95%) of the heptapeptide as a solid.

Synthesis of Boc–Val–Ala–Leu–Dpg–Val–Ala-Leu-OMe (Dpg-7)

Boc–Leu–Dpg–OMe (6). Boc–Leu–OH (4.6 g, 20 mmol) was dissolved in dichloromethane (8 mL) and cooled in an ice bath. H_2N–Dpg–OMe isolated from (5.25 g, 25 mmol) of its hydrochloride was added, followed by DCC (4.16 g, 20 mmol) and stirred for 36 h at room temperature. Dichloromethane was evaporated, the residue was diluted with ethylacetate, and DCU filtered. The solution was washed with brine (1 ×30 mL), 2N HCl (3 × 50 mL), brine (1 × 30mL), 1*M* Na_2CO_3 (3 × 50 mL), and again with brine (50 mL). The organic layer was dried over anhydrous Na_2SO_4 and evaporated under reduced pressure to afford 6.9 g (18 mmol, 94%,) of a white solid. ^{1}H-nmr (80 MHz, $CDCl_3$, δ): 0.80–0.93, 12H ($C^{\delta}H_3$ Leu/Dpg); 1.26, 1.65, 2,20, 11H (Dpg $C^{\beta}H_2/C^{\gamma}H_2$, Leu $C^{\beta}H_2/C^{\gamma}H$); 1.42, 9H, s (Boc CH_3); 3.42, 3H, s (—O—CH_3); 3.98, 1H, m (Leu $C^{\alpha}H$); 4.72, 1H, d (Leu NH); 6.80, 1H, s (Dpg NH).

Boc–Leu–Dpg–OH (7). The dipeptide ***6*** (6.2 g, 6 mmol) was saponified using 16 mL of methanol and 4 mL of 4N NaOH with stirring for 4 days at room temperature. Methanol was evaporated and the residue dissolved in water. The aqueous solution was washed with ether (2 × 15 mL), cooled in an ice bath and acidified to pH 2 with 6N HCl. The product was extracted into ethylacetate (3 × 50 mL). The ethylacetate layer was dried over anhydrous Na_2SO_4 and evaporated under reduced pressure to afford 2.85g (6.8 mmol, 85%) of the dipeptide acid as a white solid.

Boc–Leu–Dpg–Val–OMe (8). The dipeptide acid ***7*** (2.2g, 6 mmol) was coupled to H_2N–Val–OMe isolated from 1.904 g (12 mmol) of its hydrochloride using DCC (1.6 g, 8 mmol) and HOBt (0.810 g, 6 mmol) in DMF (5 mL) with stirring for 72 h at room temperature. The reaction mixture was diluted with ethylacetate and DCU filtered. The ethylacetate layer was washed with brine (50 mL), 2N HCl (3 × 30 mL), 1*M* Na_2CO_3 (3 × 30 mL) and brine (50 mL). The organic layer was dried over anhydrous Na_2SO_4 and evaporated to dryness under reduced pressure to yield 2.764 g (5.74 mmol, 95%) of a white solid. ^{1}H-nmr (80 MHz, $CDCl_3$, δ): 0.88–1.02, 18H ($C^{\delta}H_3$ Dpg/Leu, Val $C^{\gamma}H_3$); 1.53, 9H, s (Boc CH_3); 1.26, 1.65,1.70, 2.12, 14H (Dpg $C^{\gamma}H_2/C^{\beta}H_2$, Leu $C^{\beta}H_2/C^{\gamma}H$/Val $C^{\beta}H_2$/ $C^{\gamma}H$); 3.42, 3H, s (—O—CH_3); 4.05–4.35 2H, m (Leu/Val $C^{\alpha}H$); 4.72, 1H, d (Leu NH); 6.30, 1H, d (Val NH); 7.10, 1H, s (Dpg NH).

Boc–Leu–Dpg–Val–OH (9). The tripeptide ***8*** (2.425g, 5 mmol) was saponified using 5 mL of methanol and 2 mL of 2N NaOH with stirring for 2 days at room temperature. Workup of the reaction mixture as described in the case of ***2*** afforded 2.0 g (4.5 mmol, 95%) of the tripeptide acid as a white solid.

Boc–Ala–Leu–OMe (10) Boc–Ala–OH (5.67 g, 30 mmol) was coupled to H_2N–Leu–OMe isolated from 9.05g (50 mmol) of its hydrochloride using DCC (6.18 g, 30 mmol) and HOBt (4.05g, 30 mmol) in DMF with stirring for 24 h at room temperature. Work up of the reaction mixture as described in the case of ***1*** afforded 9.29 g (98%, 29.4 mmol) of a gummy solid. ^{1}H-nmr (80 MHz, $CDCl_3$, δ): 0.90, 6H ($C^{\delta}H_3$ Leu); 1.47, 3H (Ala $C^{\beta}H_3$); 1.5, 9H, s (Boc CH_3); 1.60,1.72, 3H (Leu $C^{\beta}H_2/C^{\gamma}H$); 3.70, 3H, s (—O—CH_3); 4.1–4.4, 2H ($C^{\alpha}H$ Ala/Leu); 5.1, 1H, d (Ala NH); 6.4, 1H, d (Leu NH).

H_2N–Ala–Leu–OMe (11). The dipeptide ***10*** (8.9 g, 29 mmol) was deprotected using 100 mL of 98% formic acid at room temperature. The progress of the reaction was monitored by TLC. On completion of reaction, formic acid was evaporated under reduced pressure. The residue was taken in water (100 mL) and washed with ether (2 × 30 mL). The pH of the aqueous layer was adjusted to 8 with Na_2CO_3. The product was extracted into ethylacetate (3 × 60 mL). The ethylacetate layer was dried over anhydrous Na_2SO_4 and evaporated under reduced pressure to afford 4.7g (22.6 mmol, 78%) of a gum that was ninhydrin positive.

Boc–Leu–Dpg–Val–Ala–Leu–OMe (12). The tripeptide acid ***9*** (1.772 g 4 mmol) was coupled to 8 mmol of ***11*** using DCC (0.824 g, 4 mmol) and HOBt (0.540 g, 4mmol) in DMF with stirring for five days at room temperature. Workup of the reaction mixture as described in the case of ***3*** afforded 2.484 g (3.6 mmol, 90%) of a white solid. ^{1}H-nmr (80 MHz,$CDCl_3$, δ): 0.80–0.98, 24H ($C^{\delta}H_3$, Dpg/Leu, $C^{\gamma}H_3$, Val) 1.01, 1.26, 1.52;1.67, 2.02, 18H (Dpg $C^{\beta}H_2/C^{\gamma}H_2$, Leu $C^{\beta}H_2/C^{\gamma}H$, Val $C^{\beta}H$, Ala $C^{\beta}H_3$) 1.50 9H, s (Boc CH_3); 3.63, 3H, s (—O—CH_3); 3.98, 4.12, 4H, m (Ala/Leu/Val $C^{\alpha}H$); 4.85, 1H, d (Leu [1] NH); 6.68, 1H, s (Dpg NH); 6.7–7.6, 3H (Val/Ala/Leu/NH).

H_2N–Leu–Dpg–Val–Ala–Leu–OMe (13). Deprotection of ***12*** (2.007 g, 3 mmol) was done using 12 mL of 98% formic acid for 12 h at room temperature. Workup of the reaction mixture as described in the case of ***4*** afforded 1.194g (2.1 mmol, 70%) of the free amine as a gum which was ninhydrin positive.

Boc–Val–Ala–Leu–Dpg–Val–Ala–Leu–OMe (14). Boc–Val–Ala–OH (0.432 g, 1.5mmol) was coupled to 1.194 g (2.1 mmol) of ***13*** using DCC (0.39g , 1.5 mmol) and HOBt (0.025 g, 1.5 mmol) in DMF with stirring for seven days at room temperature. Work up of the reaction mixture as described in the case of ***3*** afforded 1.157 g (1.38 mmol, 92%) of the heptapeptide as a solid.

Acetylation of Peptides (Ac–Val–Ala–Leu–Xxx–Val–Ala–Leu–OMe; Xxx = Ac_8c, Ac_7c, Aib, Dpg, Deg)

Acetyl derivatives were prepared for all the five peptides in order to facilitate acid induced unfolding studies in organic solvents and to explore crystallization . The general procedure used is given below. The peptide (0.25 mmol) was deprotected using 98% formic acid. The progress of the reaction was monitored by TLC. After completion of the reaction, formic acid was evaporated, the residue was taken in water, and washed with ether (2 × 20 mL). The aqueous layer was cooled in an ice bath and neutralized by Na_2CO_3. The free base was extracted in ethylacetate (3 × 50 mL), dried over anhydrous Na_2SO_4, and concentrated under reduced pressure to give the free base as a gum that was ninhydrin positive. This was dissolved in a 1:1 mixture of acetic acid and acetic anhydride and stirred overnight at room temperature. Water (5 mL) was added and the solution evaporated to dryness. The residue was dissolved in ethylacetate (30 mL) and the solution washed with brine (15 mL), 1N HCl (3 × 15 mL), 1*M* Na_2CO_3 (3 × 15 mL), brine (15 mL), dried over anhydrous Na_2SO_4 and concentrated under reduced pressure. Trituration with n-hexane gave a nice solid. The yields and melting points are as follows: Ac-Ac_8c-7: 72%, Ac-Ac_7c-7: 58%, 197°C; 204°C; Ac-Aib-7: 64%, 184°C; Ac-Dpg-7: 68%, 195°C; Ac-Deg-7: 60%, 192°C.

Spectroscopic Studies

All nmr experiments were carried out on Bruker AMX-400 and DRX-500 spectrometers at the Sophisticated Instrumentation Facility, Indian Institute of Science, Bangalore. All nmr spectra were recorded at a peptide concentration of 3 m*M* in both $CDCl_3$ and DMSO. All two-dimensional (2D) data were acquired at 1K data points, 512 experiments, with 48–64 transients. A 300 ms mixing time was used for ROESY experiments. The spectral width for all the experiments was set to 4500 Hz. Nuclear magnetic resonance data were processed using XWINNMR software. All two dimen-

Table II Crystal and Diffraction Parameters[a]

	Dpg-7	Ac-Dpg-7
Empirical formula	$C_{42}H_{76}N_7O_{11}H_2O$	$C_{39}H_{70}N_7O_9$
Crystallizing solvent	CH_3OH/H_2O	CH_3OH/H_2O
Cocrystallized solvent	H_2O	
Color/habit	Colorless thin plate	Very thin, fragile colorless wafers
Crystal size (mm)	$0.12 \times 0.25 \times 0.55$	$0.13 \times 0.18 \times 0.55$
Space group	$P2_1\ 2_1\ 2_1$	$P2_1$
a (Å)	12.138(3)	10.705(3)
b (Å)	16.015(1)	17.567(7)
c (Å)	27.112(3)	13.584(4)
β (deg)	90.0	112.98
V (Å^3)	5270	2351.8
Z	4	2
Mol. wt.	855.1	781.0
Density (calc; g/cm^3)	1.078	1.103
$F(000)$	1860	850
T (°C)	21	21
No. of unique reflections	4534	3575
No. of obs. rflns., $\lvert F_0\rvert > 4\sigma F$	2349	2154
Final R_1 (obs. data; %)	9.13	15.6
S	1.02	1.05
Resolution (Å)	0.9	0.9
Data/param. ratio	4.2:1.0	4.3:1.0
No. of param.	561	496

[a] For both crystals, CuK_α radiation ($\lambda = 1.54178$ Å) was used with a $\theta/2\theta$ scan, a scan width of $2.0° + 2\theta(\alpha_1 - \alpha_2)$, and a scan speed of 10 deg/min. Standard reflections were read after every 97 measurements. Standards remained constant (within 3%).

sional data sets were zero filled to 1024 points with a 90° phase-shifted squared sine-bell filter in both dimensions. The probe temperature was maintained at 300 K.

Crystallization and X-Ray Diffraction

Crystals for both Dpg-7 and Ac-Dpg-7 grew as thin plates with many small inclusions. Crystals for Ac-Dpg-7, and to a smaller extent for Dpg-7 were in the form of very thin, fragile wafers that adhered to each other tenaciously. The crystals used for data collection were most likely a composite of several individual wafers that were sufficiently well aligned to give a reasonable sharp optical extinction under crossed Nicol prisms. However, the profiles of the diffraction spots showed peaks with multiple maxima. These defects in the single "crystals" available for data collection contributed to the poor values for the crystallographic R-factors.

The x-ray diffraction data were measured on a Siemens P4 automated four-circle diffractometer (presently called Bruker) equipped with a graphite monochromator. For both crystals $CuK\alpha$ radiation ($\lambda = 1.54178$ Å) was used with a $\theta/2\theta$ scan, a scan width of $2.0° + 2\theta$ (α1-α2) and a scan speed of 10 deg/min. Three check reflections were read after every 97 measurements. The standards remained constant within 3%. Crystal and diffraction parameters are listed in Table II.

The structure of A-Dpg-7 was solved routinely by direct phasing methods, while the Dpg-7 structure required 1000 trials of direct phasing in the TREF routine found in the SHELXTL package of programs.[36] Full-matrix least-squares refinements with anisopropic thermal parameters were performed on the coordinates of C, N, and O atoms. Hydrogen atoms were placed in idealized positions and allowed to ride with the C or N atoms to which each is bonded. The side chains for Leu and Val residues had considerable positional motion, especially near the C-terminals, as evidenced by large values for the thermal factors for atoms in the side chains. The imperfect crystals may have enhanced this effect; however, in view of the conformational fragility observed in the model heptapeptide Boc–Val–Ala–Leu–Aib–Val–Ala–Leu (Aib-7),[18,19] where Aib is replaced by Dpg in the present compounds, the large thermal parameters were not unexpected. For the least-squares refinement, restraints were placed on distances in the Leu (7) side chain in both Dpg-7 and Ac-Dpg-7, as well as on the Val(5) side chain in Ac-Dpg-7. Initially, least-squares refinements using F data with $\lvert F\rvert > 4\sigma$ were used, followed by refinements with F^2 data using all the observed data. There was no significant difference in the results. The results from the F^2 refinement are reported.

Fractional coordinates for Dpg-7 and Ac-Dpg-7 are deposited in the Cambridge Crystallographic Data Base.

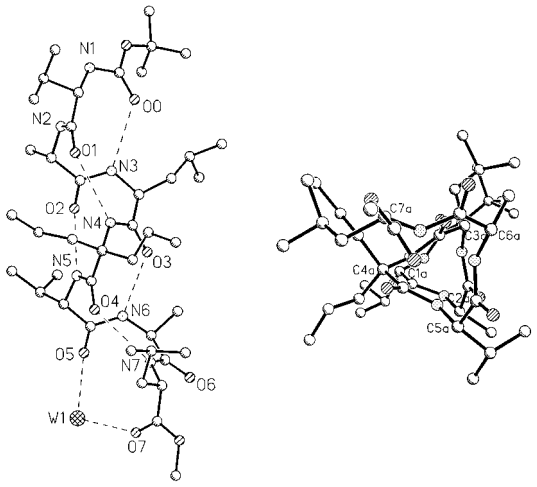

FIGURE 1 Views of the 3_{10}-helix adopted by (Boc)-Dpg-7. The left view is directed perpendicularly to the helix axis. Dashed lines indicate the NH· · ·O hydrogen bonds. A water molecule W1 forms hydrogen bonds with carbonyl O5 and carbonyl O7 at the partially unwound C-terminus. The right view, directed into the interior of the helix, shows the characteristic triangular projection of a 3_{10}-helix backbone.

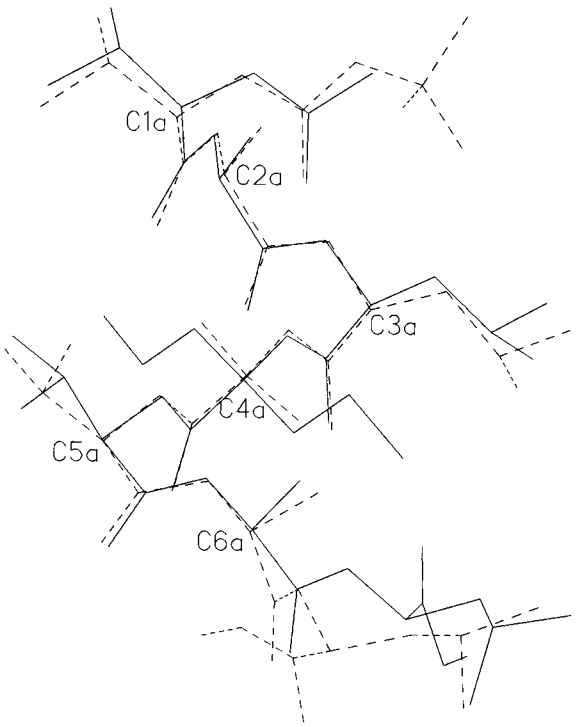

FIGURE 3 Superposition of the α-helical conformations of Ac-Dpg-7 (this paper; solid line) and Aib-7A.[18] The differences in the heptapeptide analogues are Ac/Boc and Dpg^4/Aib^4 in Ac-Dpg-7 and Aib-7A, respectively.

RESULTS AND DISCUSSION

Crystal State Conformations

Crystal structures determined for the Boc and acetyl derivatives of the Dpg heptapeptide (Dpg-7 and Ac-Dpg-7).are shown in Figures 1 and 2, each displaying two views of the molecular conformations. Although both peptides adopt helical structures, the Boc analogue adopts a 3_{10}-helix with $4 \rightarrow 1$ hydrogen bonds, except for some unwinding at the C-terminus, while the Ac analogue forms a good α-helix. It is noteworthy that Aib-7A[18] is almost identical to Ac-Dpg-7, rather than to Dpg-7. A superposition of Aib-7A and Ac-Dpg-7, made with a least-squares fit of backbone atoms from N1 to C6a, shows an excellent fit between the two molecules from the N-terminus (despite having an Ac group in one and a Boc group in the other) to C6a (Figure 3), and despite the high *R* factor for Ac-Dpg-7. Differences occur at the C-terminus, but they are not sufficient to disturb the N7—O3 hydrogen bond (α-helical) at 2.92 Å for Ac-Dpg-7 and 3.02 Å for Aib-7A. Backbone torsion angles and hydrogen-bond parameters are summarized in Tables III and IV, respectively.

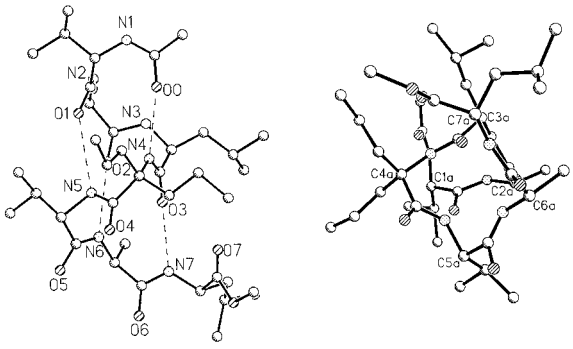

FIGURE 2 Views of the α-helix adopted by Ac-Dpg-7. In the left view, dashed lines indicate the NH· · ·O hydrogen bonds. The right view, directed into the interior of the helix, shows a square projection for the backbone segment C2a to C7a, characteristic of an α-helix.

The facile transition between a 3_{10}-helix in the backbone of Dpg-7 and an α-helix in the backbone of Ac-Dpg-7, both crystallized from the same solvent and both having the same sequence, except for the N-terminal end groups, is indicative of both having similar conformational energies. The different helix forms for the backbone cannot be attributed to the change in end group from Boc to Ac. Pairs of analogues in which the N-terminus has been changed but in which the conformation remains the same are, for example, as follows: (Boc)-Aib-7A[18,19] and Ac-Dpg-7 (this paper) wherein Dpg(4) replaces Aib(4) as well as Ac replaces Boc; and the pair Ac(Aib–Val–

Table III Torsion Angles (degrees)[a]

Residue	Angle	Dpg-7	Ac-Dpg-7	Aib-7A[18]	Aib-7B[18]	Aib-7[19] (DMSO/i-PrOH)
Val(1)	ϕ	−60	−61	−71	−70	−75
	ψ	−30	−53	−41	−45	−36
	ω	−176	180	−178	−172	177
	χ^1	−175	178	−179	178	179
		−75	−65	−57	−61	−56
Ala(2)	ϕ	−72	−55	−61	−65	−76
	ψ	−2	−43	−45	−45	−44
	ω	170	180	179	179	−179
Leu(3)	ϕ	−57	−62	−71	−68	−62
	ψ	−22	−48	−35	−38	−29
	ω	179	−176	180	−177	−179
	χ^1	−78	−175	−169	−176	−151,−79
	χ^2	−59	68	61	57	−178,55
		180	−169	−176	−177	−53,−175
Xxx(4)	ϕ	−52	−52	−57	−56	−59
	ψ	−29	−39	−35	−40	−28
	ω	−175	−176	−178	−173	−176
	χ^1	−170[b], 52[c]	−173, 61[c]			
	χ^2	−176, 177	164, −173			
Val(5)	ϕ	−71	−80	−87	−91	−109
	ψ	−7	−27	−11	2	17
	ω	178	−179	173	179	−180
	χ^1	71	−74	64	67	60
		−56	161	−61	−58	−63
Ala(6)	ϕ	−89	−90	−78	−73	−102
	ψ	1	−56	−41	−36	153
	ω	180	−169	−175	−177	169
Leu(7)	ϕ	−65	−145	−127	−134	−86
	ψ	153	150	10	−22	159
	ω	172	179	176	−178	176
	χ^1	−76	−82	−67	−65	−63
	χ^2	180	−173	171	174	174
		−67	−45	−62	−63	−65

[a] Torsion angles follow the IUPAC-IUB Commission on Biochemical Nomenclature.[46] The last 3 columns list values determined earlier for the peptide Boc–Val–Ala–Leu–Aib–Val–Ala–Leu–OMe (Aib-7) in polymorphic forms. Aib-7A/Aib-7B refers to two molecules in the asymmetric unit of a $P2_1$ cell.

[b] One propyl side chain is disordered with the other conformation having $\chi^1 = 66$ and $\chi^2 = 170$.

[c] Other propyl side chain.

Ala–Leu)$_2$OMe and Boc(Aib–Val–Ala–Leu)$_2$OMe[37] with different crystal packing but the same conformation for the molecules. The factors causing the conformational fragility in the heptapeptides containing one Aib or Dpg residue at position 4, that is, helix transitions, water insertion and unfolding of the backbone,[18,19] shown in Figure 4, are not yet adequately defined.

The solid state structures demonstrate that a single centrally located Dpg residue stabilizes fully helical conformations in a manner entirely analogous to the case of Aib residue. Despite the possibility of fully extended conformation at Dpg, very few examples of Dpg in nonhelical conformations have so far been observed in crystal structures of heteromeric peptide sequences.[29,31]

NMR Assignments

Sequence specific ^{1}H-nmr assignments were readily achieved for all the five peptides using a combination of 2D correlated spectroscopy (COSY) and rotating frame nuclear Overhauser effect spectroscopy (ROESY) experiments. The relevant chemical shifts of the backbone NH and C$^\alpha$H protons for the peptides in $CDCl_3$ and $(CD_3)_2SO$ are summarized in Table V.

Table IV Hydrogen Bonds

Dpg-7				Ac-Dpg-7			
Type	Donor	Acceptor	N···O (Å)	Type	Donor	Acceptor	N···O (Å)
Head to tail	N1	O5	2.99	Head to tail	N1	O4	2.98
Head to tail	N2	W1	2.93	Head to tail	N2	O5	2.96
4 → 1	N3	O0	3.15		N3	O0	3.18[a]
4 → 1	N4	O1	3.22	5 → 1	N4	O0	2.94
4 → 1	N5	O2	3.05	5 → 1	N5	O1	3.27
4 → 1	N6	O3	2.95	5 → 1	N6	O2	3.17
4 → 1	N7	O4	3.27	5 → 1	N7	O3	2.92
Solvent–peptide	W1	O5	2.75				
Solvent–peptide	W1	O7	2.81				

[a] N(3)H···O0 = 2.76 Å, too long for a good hydrogen bond.

Inspection of the chemical shifts reveals that all five peptides have an extremely similar distribution of NH and $C^{\alpha}H$ chemical shifts in $CDCl_3$, suggesting close identity of the backbone conformations in this solvent. In contrast, in $(CD_3)_2SO$, the observed pattern of chemical shifts is very similar for the Ac_8c, Ac_7c, and Aib peptides, while marked differences are observed for the Dpg and Deg peptides. Particularly noteworthy are the large downfield shifts of the Leu(3) and Val(5) NH resonances in the Dpg and Deg peptides and the upfield shift of the Xxx(4) NH. A small but significant upfield shift is also noted for the Leu (3) $C^{\alpha}H$ resonance in the Dpg and Deg peptides.

Delineation of Solvent-Shielded NH Groups

Figure 5 shows the effect of addition of a hydrogen-bonding solvent DMSO to solutions of peptides in an apolar solvent $CDCl_3$. At low concentrations (~20% v/v) of the perturbant DMSO, only the Val(1) and Ala(2) NH groups show appreciable downfield shifts in the four peptides studied. (Ac_8c-7, Ac_7c-7, Dpg-7, and Deg-7). Similar results have earlier been obtained for the Aib analogue.[19] At higher DMSO concentration, significant differences are observed between the Ac_nc peptides on the one hand and the Dxg peptides on the other. In the case of the Dxg peptides, Leu(3) NH, Val(5) NH, and Leu(7) NH also show appreciable downfield shifts with increase in DMSO concentration. The discontinuous solvent titration curves observed for the Dxg analogues is strongly suggestive of a solvent-dependent conformational transition. At low DMSO concentrations, largely helical structures are populated in which only two NH groups Val(1) and Ala(2) are available for solute–solvent hydrogen bonding. Beyond a DMSO concentration of 20%, a significant population of unfolded structures is obtained in the case of the Dxg analogues, rationalizing the increased exposure of the Leu(3), Val(5) ,and Leu(7) NH groups. Careful examination of the curves in Figure 5 reveals that helix fragility in DMSO may also be a feature in the case of the Ac_nc analogues, although the effects are much less pronounced than in the Dxg peptides.

Solvent shielding of NH groups in DMSO was probed by measuring the temperature coefficients ($d\delta/dt$) of NH chemical shifts. Since DMSO interacts strongly with exposed NH groups, higher temperature coefficients are expected for free NH groups in peptides, while intramolecularly hydrogen-bonded NH groups exhibit low temperature coefficients. While quantitative interpretation of $d\delta/dt$ magnitudes is risky, nevertheless wide variations in $d\delta/dt$ values within the same peptide afford a delineation of exposed and buried NH groups. Figure 6 provides the comparison of the $d\delta/dt$ values observed in the five peptides. The solvent-dependent chemical shift [$\Delta\delta$

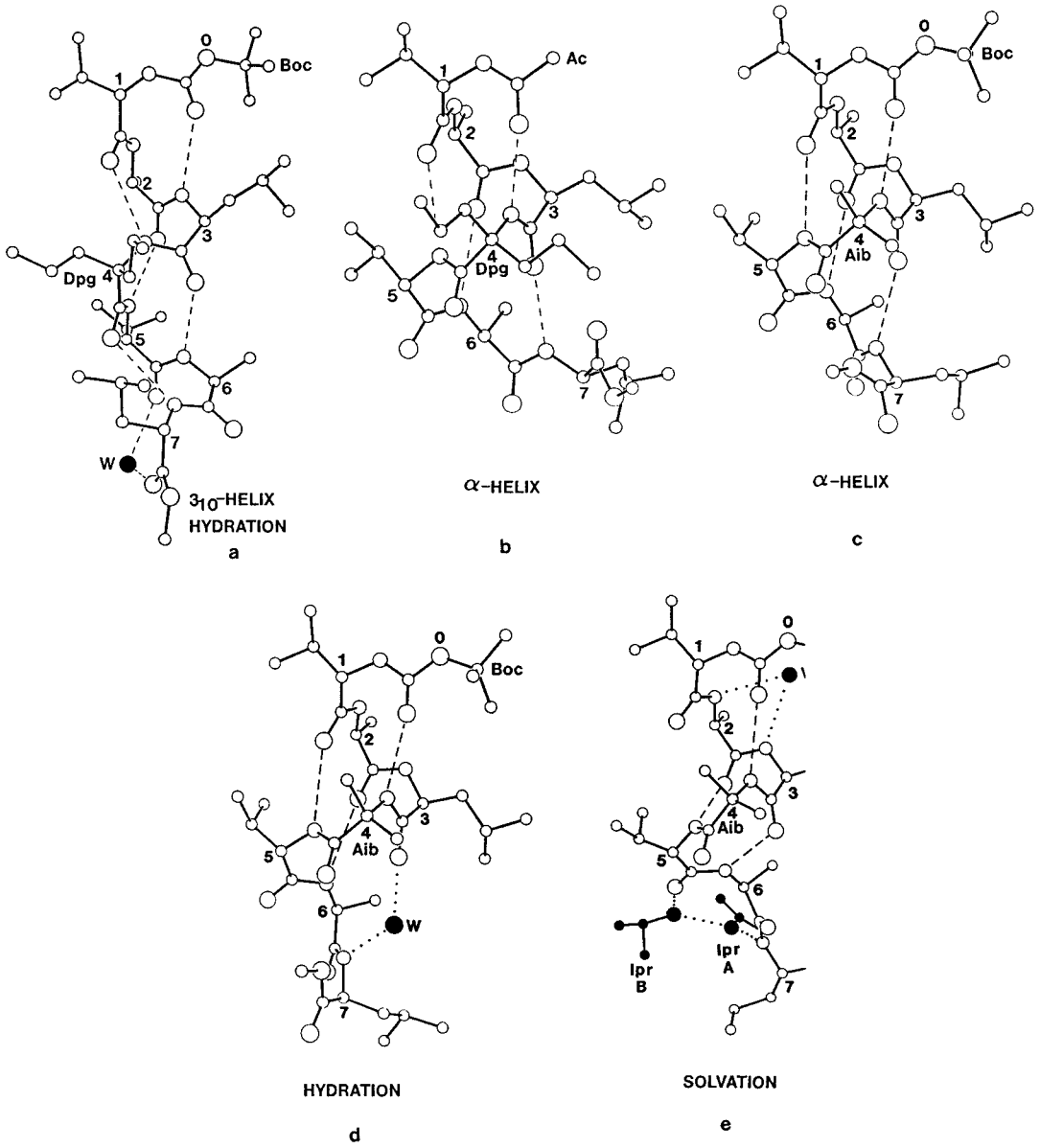

FIGURE 4 Comparison of conformations for five analogues of (Ac/Boc)–Val–Ala–Leu–(Dpg/Aib)–Val–Ala–Leu–OMe. (a) A 3_{10}-helix with a water molecule insertion into the backbone near the C-terminus. (b) and (c) α-Helices with two changes of residues between them. (d) α-Helix with water insertion into backbone [occurring in same crystal as (c)].[18] The water insertion is in a different place than in analogue (a). (e) Distorted and frayed helix crystallized from DMSO/isopropanol solution. DMSO did not cocrystallize, but two molecules of IprOH and one water molecule did make hydrogen bonds with backbone atoms.[19]

$= \delta(CD_3)_2SO - \delta CDCl_3]$, which is also a measure of the degree of solvent exposure, is summarized in Figure 7. The $d\delta/dt$ values clearly reveal important differences between the peptides. The relatively high $d\delta/dt$ values observed in DMSO for most of the NH resonances suggest that fully folded helical conformations are poorly populated in this strongly interacting solvent. This is unsurprising since DMSO acts as a strong hydrogen-bond acceptor and competes for peptide NH groups. Particularly noteworthy are the $d\delta/dt$ values observed for the Xxx(4) and Val(5) NH groups. In the case of the Aib and Ac_nc peptides, a low $d\delta/dt$ value (1.2–1.5 ppb/K) is observed for Val(5) NH, while a relatively high value (4.8–5.5 ppb/K) is observed for the Xxx(4) NH. In sharp contrast, exactly the opposite is observed for the Dxg

Table V NMR Parameters for the Peptides Boc–Val–Ala–Leu–Xxx–Val–Ala–Leu–OMe

Chemical Shifts in $CDCl_3$ (δ, ppm)

Xxx → Residue ↓	NH					$C^{\alpha}H$				
	Ac_8c	Ac_7c	Aib	Dpg	Deg	Ac_8c	Ac_7c	Aib	Dpg	Deg
Val(1)	5.44	5.39	5.34	5.32	5.21	3.72	3.72	3.77	3.72	3.73
Ala(2)	6.83	6.85	6.78	6.76	6.70	4.18	4.15	4.16	4.15	4.19
Leu(3)	7.27	7.31	7.30	7.28	7.27	4.19	4.11	4.09	4.12	4.13
Xxx(4)	7.24	7.26	7.49	7.27	7.22	—	—	—	—	—
Val(5)	6.75	6.84	6.87	6.77	6.75	4.20	4.18	4.19	4.19	4.21
Ala(6)	7.62	7.57	7.65	7.74	7.72	4.55	4.49	4.50	4.47	4.51
Leu(7)	7.20	7.23	7.27	7.21	7.17	4.56	4.56	4.56	4.52	4.55

Chemical Shifts in $(CD_3)_2SO$ (δ, ppm)

Xxx → Residue ↓	NH					$C^{\alpha}H$				
	Ac_8c	Ac_7c	Aib	Dpg	Deg	Ac_8c	Ac_7c	Aib	Dpg	Deg
Val(1)	6.77	6.75	6.76	6.73	6.73	3.79	3.78	3.78	3.77	3.78
Ala(2)	7.93	7.92	8.00	7.86	7.85	4.26	4.27	4.26	4.33	4.35
Leu(3)	7.95	7.97	7.91	8.32	8.35	4.29	4.29	4.29	4.06	4.10
Xxx(4)	7.84	7.85	8.08	7.57	7.54	—	—	—	—	—
Val(5)	6.99	6.94	7.07	7.66	7.66	4.04	4.04	4.05	4.05	4.07
Ala(6)	7.84	7.78	7.98	7.89	7.92	4.22	4.25	4.25	4.27	4.28
Leu(7)	7.88	8.11	8.10	7.90	7.87	4.25	4.26	4.26	4.26	4.24

peptides, with Xxx(4) NH having a low $d\delta/dt$ value (2.4– 2.5 ppb/K), whereas Val(5) has a very high $d\delta/dt$ value (8.2 ppb/K).

A possible interpretation for this observation is that the Leu(3)–Xxx(4) β-turn conformation remains highly populated in DMSO for the Aib and Ac_nc peptides. This would result in strong solvent shielding of the Val(5) NH, which would be involved in an intramolecular 4 → 1 hydrogen bond. Type III β-turns indeed correspond to isolated 3_{10}-helical turns and have been commonly observed in Aib[2,39] and Ac_nc peptides.[20,22,39,40] The high $d\delta/dt$ value for Val (5) NH in the Dxg peptides clearly argues against such structures. The low $d\delta/dt$ value for the Xxx(4) NH may be a consequence of a population of fully extended C_5 structures at the Dxg residue. It should be noted that in these fully extended conformations, the Xxx(4) NH group is proximal to the Xxx(4) CO group, a feature that should result in inhibition of solvation by DMSO as a consequence of stereoelectronic factors. The approach of the sulfoxide would be energetically repulsive in the vicinity of the CO group.[34]

The Δδ values summarized in Figure 7 are more complicated to interpret since the nature of the major conformers is dramatically altered on going from $CDCl_3$ to DMSO. Nevertheless, the distribution of Δδ values across the length of the peptide chain clearly allows grouping of the peptides into two classes. The Aib and Ac_nc analogues belong to one family, while the Dxg analogues belong to a second family. The classification is most clearly manifested in the behavior of the Leu(3), Xxx(4), and Val(5) NH groups.

In the case of the Aib and the Ac_nc analogues, Val(5) has a very low Δδ value, whereas in the Dxg series this resonance shows a large downfield shift on going from $CDCl_3$ to DMSO. The situation is reversed in the case of the Xxx(4) NH where a moderate Δδ value (~0.6 ppm) is noted for the Aib and Ac_nc analogues, while a significantly lower value of ~0.3 ppm is observed for the Dxg peptides. Such a differentiation is also observed for the Leu(3) NH, with the Dxg peptides showing a much larger solvent shift than the Aib/Ac_nc analogues, although in all cases a relatively high value of Δδ is observed.

The nmr data described thus far suggest that in an apolar solvent like $CDCl_3$, all five peptides adopt predominantly helical conformations with the NH groups of residues 3–7 being involved in intramolecular hydrogen bonds. The only nonhydrogen-bonded NH groups are those of Val(1) and Ala(2). Both 3_{10}- and mixed $3_{10}/\alpha$-helical structures involving bifur-

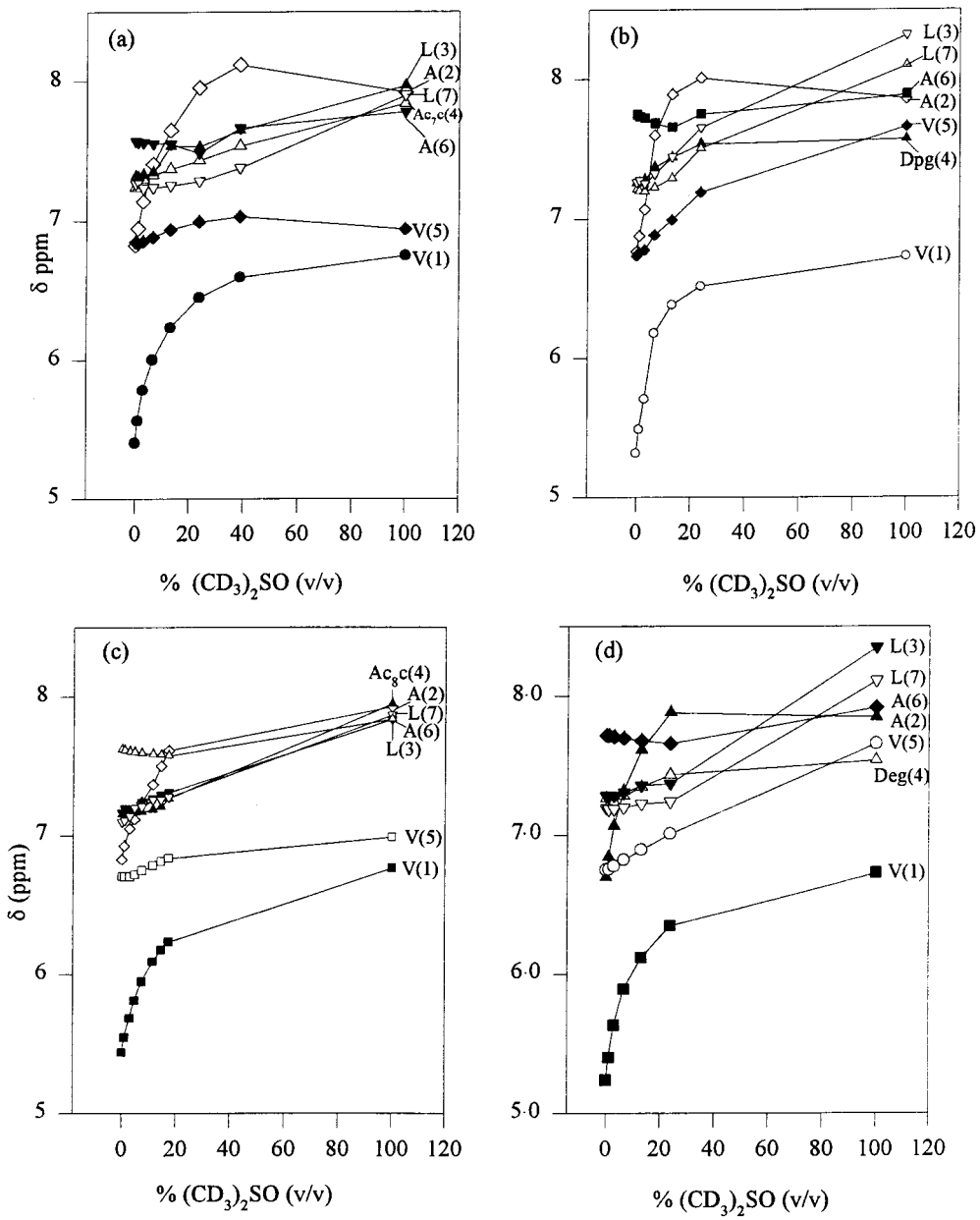

FIGURE 5 Solvent dependence of NH chemical shifts for the peptides Boc–Val–Ala–Leu–Xxx–Val–Ala–Leu–OMe in $CDCl_3$–$(CD_3)_2SO$ mixtures at varying composition [Xxx = (a) Ac_7c, (b) Dpg, (c) Ac_8c and (d) Deg].

cated hydrogen bonds at the N-terminus are consistent with the nmr data. Inspection of the crystal structure of the Dpg containing heptapeptides [Figures 1 and 2 and Tables 3 and 4] reveal that the NH groups of residues 3–7 are indeed involved in intramolecular hydrogen bonding. It is therefore reasonable to conclude that the predominant conformation in a noninteracting solvent like $CDCl_3$ resembles the structure observed in crystals. Most notably, all five peptides show similar solution properties in $CDCl_3$, suggesting that the nature of the Xxx(4) residue does not significantly affect the conformational distribution. CD spectra recorded for all five peptides in methanol were also largely similar (data not shown), exhibiting a weak negative band at ~220 nm and a strong negative band at ~205 nm, a feature of short helical peptides.[41]

In a strongly solvating medium like DMSO, which can compete with peptide carbonyl groups for hydrogen bonding to NH groups, the situation appears distinctly different. In DMSO, the observed nmr param-

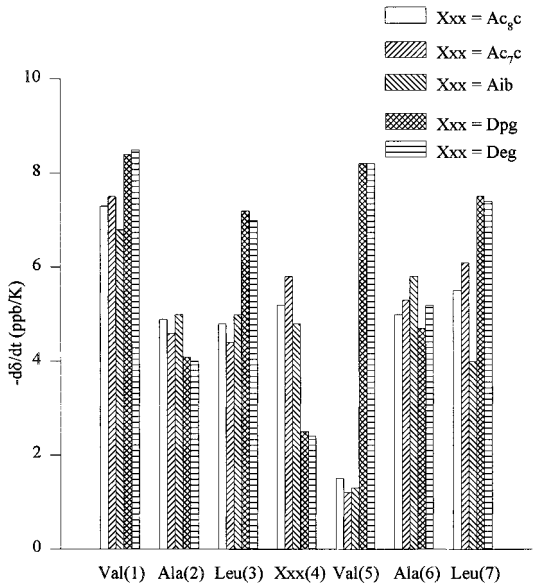

FIGURE 6 Bar diagram showing the temperature induced perturbation of NH chemical shifts for the peptides Boc–Val–Ala–Leu–Xxx–Val–Ala–Leu–-OMe (Xxx = Ac_8c, Ac_7c, Dpg and Deg). The $d\delta/dt$ is the temperature coefficient in $(CD_3)_2SO$.

eters clearly point to differences in the behavior of the Dxg and Aib/Ac_nc containing peptides. The stereochemical influence of the amino acids with cycloalkane side chains appears to be similar to the prototype residue Aib. In contrast, residues with linear alkyl side chains, Dxg, lead to a different conformational distribution resulting in distinctive chemical shift and temperature coefficient patterns. The nmr data suggests that in all the five peptides the degree of solvent exposure of NH groups of residues 3 – 7 is clearly greater than in the case of $CDCl_3$. This is consistent with the greater fragility of the peptide helix in a strongly solvating environment.[19,34] While the data supports residual helical conformations, in the case of the Aib and Ac_nc peptides, the Dxg analogues may in fact favor more extended conformations.

Nuclear Overhauser Effects

Interresidue nuclear Overhauser effects (NOEs) between backbone protons ($C_\alpha H$, NH) can provide a useful diagnostic for the nature of the distribution of backbone conformation in solution.[42] Observation of a series of N_iH to $N_{i+1}H$ (d_{NN}) NOEs and the absence of intense $C^\alpha H$ to $N_{i+1}H$ ($d_{\alpha N}$) NOEs is a clear indicator for a predominance of helical conformations. Conversely, the absence of strong d_{NN} NOEs and the presence of intense $d\alpha_N$ NOEs are suggestive of extended conformations, with ψ values of 120 $\pm$ 60. In small peptides, heterogeneity of conformations in solution is a common occurrence, with the result that most often d_{NN} and $d_{\alpha N}$ NOEs of moderate intensity are simultaneously observed. Such a feature is interpreted as indicative of the coexistence of both helical and extended forms. NOEs were determined for the Ac_7c and Dpg peptides in both $CDCl_3$ and DMSO. ROESY experiments were used to avoid the problem of vanishingly small NOEs in the $\omega_{\tau c} \sim 1$ region.[43] In $CDCl_3$, all the sequential d_{NN} connectivities were clearly detected over the entire length of the sequence in both Ac_7c and Dpg peptides. Most $d_{\alpha N}$ NOEs were absent or very weak. Thus, the presence of a population of predominantly helical conformations for both the Dpg and Ac_7c peptides is confirmed.

In DMSO, sequential d_{NN} and $d_{\alpha N}$ NOEs were observed over the entire length of the sequence for both the peptides supporting mixed conformer populations. Inspection of the ROESY spectra suggests that $d_{\alpha N}$ NOEs are more intense than d_{NN} NOEs in the case of the Dpg peptide as compared to the Ac_7c peptide. This is suggestive of a greater population of extended conformations in the case of the Dpg analogue. Helical conformations in peptides also bring into proximity backbone protons of residues that are not adjacent in the sequence. NOEs of the type $C_i^\alpha H \leftrightarrow N_{i+2}H$ may also be observed. In ideal 3_{10}- and α-helical conformations the $d_{\alpha N}$ $(i, i + 2)$ distances are 3.8 and 4.4 Å, respectively.[42] Figure 8 shows a partial ROESY spectrum for the Ac_7c peptide in DMSO, which clearly illustrates the observation of Leu(3) $C^\alpha H \leftrightarrow$ Val(5) NH NOE, arguing for a sub-

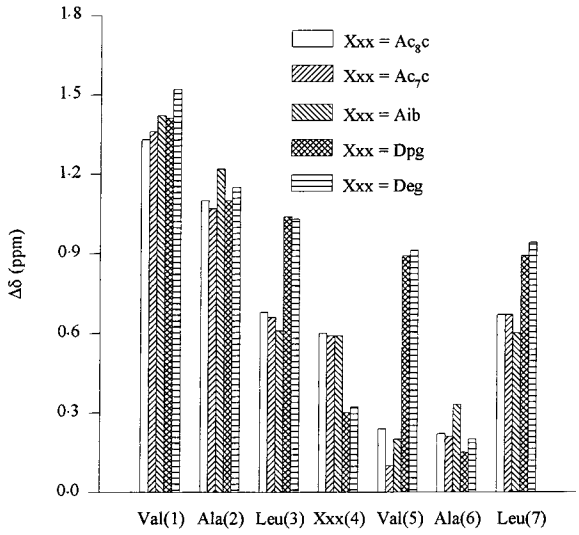

FIGURE 7 Bar diagram showing the solvent induced perturbation of NH chemical shifts for the peptides Boc–Val–Ala–Leu–Xxx–Val–Ala–Leu–OMe (Xxx = Ac_8c, Ac_7c, Dpg, and Deg). $\Delta\delta = \delta(CD_3)_2SO - \delta CDCl_3$.

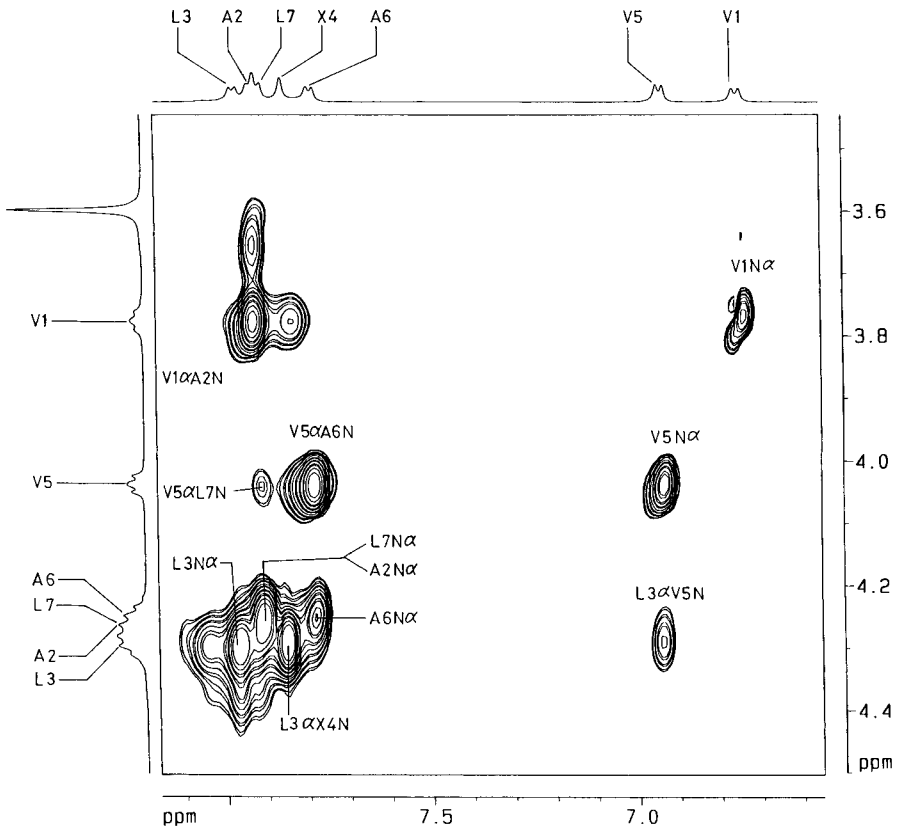

FIGURE 8 Partial 500 MHz ROESY spectrum of Boc–Val–Ala–Leu–Ac_7c–Val–Ala–Leu–OMe in $(CD_3)_2SO$ showing $C^{\alpha}H \leftrightarrow$ NH NOEs (X = Ac_7c).

stantial population of local helical conformations at the $Ac_7c(4)$ residue. A second medium-range NOE, V(5) $C^{\alpha}H \leftrightarrow$ Leu(7) NH is also detected. In contrast, these NOEs are not observed in the case of the Dpg peptide (Figure 9). The NOE results provide further support for a greater population of helical conformations in the case of the Ac_7c peptide as compared to the Dpg peptide. Since NOEs are normally observed only to distances of $\leq$4.0 Å in small peptides, the observation of the $d_{\alpha N}(i, i + 2)$ NOEs is suggestive of α-helical conformations in the Ac_7c peptide. Transitions between 3_{10}- and α-helical conformations have indeed been postulated in short Aib-containing peptides on going from $CDCl_3$ to DMSO.[12,44,45]

The results of the present study establish that α,α-dialkylated amino acids bearing linear and cyclic hydrocarbon side chains can stabilize helical conformations in short peptides in apolar solvents like $CDCl_3$. Although theoretical calculations suggest that fully extended conformations may be slightly lower in energy than helical conformations for an isolated Dxg residue, crystal structures of the two derivatives of a heptapeptide sequence containing a single Dpg residue reveal helical conformations in both cases. Clearly, intramolecular hydrogen-bond formation in helical conformations may tilt the balance in favor of helical ϕ,ψ values in Dxg peptides in apolar solvents. In crystals, facile packing of peptide helices may also provide a further means of conformational selection. In a strongly solvating medium like DMSO, however, the evidence presented in this paper suggests that helices are more favored in the case of Aib and Ac_nc peptides, while nonhelical, extended forms are more populated in the Dxg-containing sequences. Thus, helices containing Dxg residues may be more susceptible to unfolding in media that can provide competing hydrogen-bonding interactions.

This research was supported in part by grants from the Department of Science & Technology, Government of India, the National Institute of Health (grant GM-30902), and the Office of Naval Research.

NMR spectra were recorded at the Sophisticated Instrumentation Facility, Indian Institute of Science, Bangalore, India.

FAB Mass Spectra were recorded at the Regional Sophisticated Instrumentation Centre, Central Drug Research Institute, Lucknow, India.

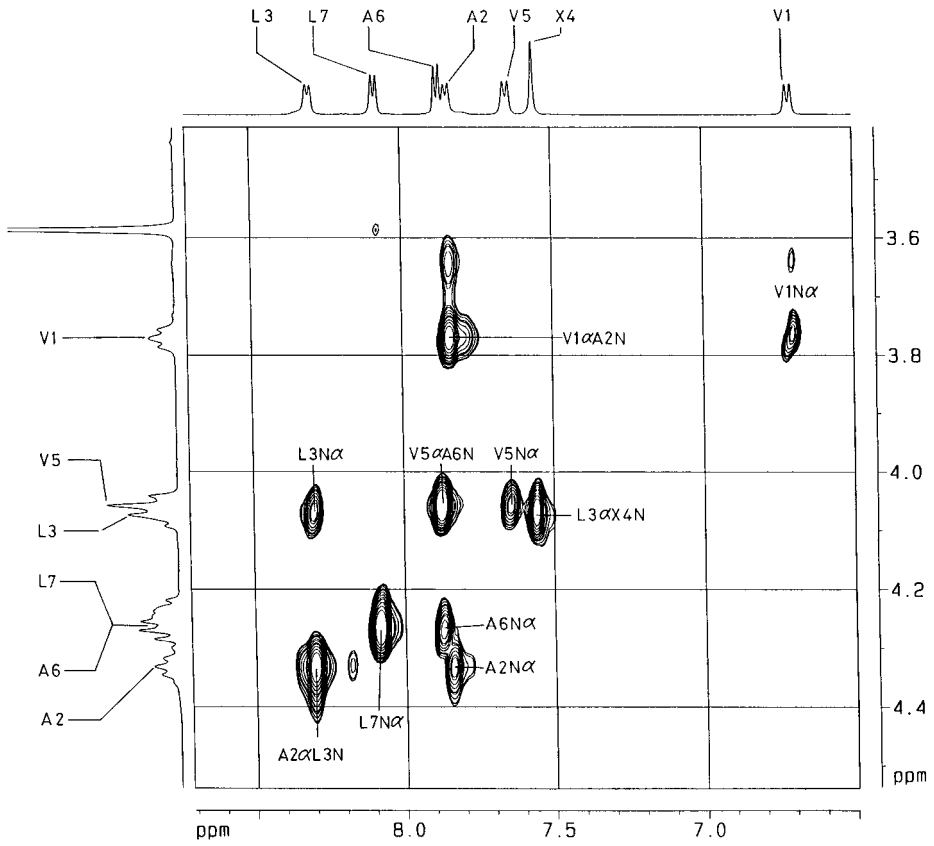

FIGURE 9 Partial 500 MHz ROESY spectrum of Boc–Val–Ala–Leu–Dpg–Val–Ala–Leu–OMe in $(CD_3)_2SO$ showing $C^{\alpha}H \leftrightarrow NH$ NOEs (X = Dpg).

REFERENCES

1. Marshal, G. R.; Bosshard, H. E. Circ Res 1972, 30/31(Suppl II),143–150.
2. Prasad, B.V. V.; Balaram, P. CRC Crit Rev Biochem 1984, 16, 307–348.
3. Nagaraj, R.; Balaram, P. Acc Chem Res 1981, 14, 356–362.
4. Mathew, M. K.; Balaram, P. Mol Cell Biochem 1983, 50, 47–64.
5. Sansom, M. S. P. Quart Rev Biophys 1993, 26, 365–421.
6. Toniolo, C.; Bonora, G. M.; Barone, V.; Bavoso, A.; Benedetti, E.; Di Blasio, B.; Grimaldi, P.; Lelj, F.; Pavone, C.; Pedone, C. Macromolecules 1985, 18, 895–902.
7. Karle, I. L.; Balaram, P. Biochemistry 1990, 29, 6747–6756.
8. Di Blasio, B.; Pavone, V.; Saviano, M.; Lombardi, A.; Nastri, F.; Pedone, C.; Benedetti, E.; Crisma, M.; Anzolin, M.; Toniolo, C. J Am Chem Soc 1992, 114, 6273–6278.
9. Karle, I. L.; Flippen-Anderson, J. L.; Gurunath, R.; Balaram, P. Protein Sci 1994, 3, 1547–1555.
10. Augspurger, J. D.; Bindra, V. A.; Scheraga, H. A.; Kuki, A. Biochemistry 1995, 34, 2566–2576.
11. Marshal, G. R.; Hodgkin, E. E.; Lansi, D. A.; Smith, G. D.; Zabrocki, J.; Leplawy, M. T. Proc Natl Acad Sci USA 1990, 87, 487–491.
12. Banerjee, A.; Datta, S.; Pramanik, A.; Shamala, N.; Balaram, P. J Am Chem Soc 1996, 118, 9477–9483.
13. Narita, M.; Doi, M.; Sugasawa, H.; Ishikawa, K. Bull Chem Soc Jpn 1985, 58, 1473–1479.
14. Narita, M.; Ishikawa, K.; Sugasawa, H.; Doi, M. Bull Chem Soc Jpn 1985, 58, 1731–1737.
15. Moretto, V.; Crisma, M.; Bonora, G.; Toniolo, C.; Balaram, H.; Balaram, P. Macromolecules 1989, 22, 2939–2944.
16. Karle, I. L.; Flippen-Anderson, J. L.; Sukumar, M.; Uma, K.; Balaram, P. J Am Chem. Soc 1991, 113, 3952–3956.
17. Karle, I. L.; Banerjee, A.; Balaram, P. Folding and Design 1997, 2, 203–210.
18. Karle, I. L.; Flippen-Anderson, J. A.; Uma, K.; Balaram, P. Proteins Struct Funct Genet 1990, 7, 62–73.
19. Karle, I. L.; Flippen-Anderson, J. L.; Uma, K.; Balaram, P. Biopolymers 1993, 33, 827–837.
20. Paul, P. K. C.; Sukumar, M.; Bardi, R.; Piazzesi, A. M.; Valle, G.; Toniolo, C.; Balaram, P. J Am Chem Soc 1986, 108, 6363–6370.

21. Barone, V.; Lelj, F.; Bavoso, A.; Di Blasio, B.; Grimaldi, P.; Pavone, V.; Pedone, C. Biopolymers 1985, 24, 1759–1767.
22. Valle, G.; Crisma, M.; Toniolo, C.; Sudhanand, Rao, R. B.; Sukumar, M.; Balaram, P. Int J Peptide Protein Res 1991, 38, 511–518.
23. Moretto, V.; Formaggio, F.; Crisma, M.; Bonora, G. M.; Toniolo, C.; Benedetti, E.; Santini, A.; Saviano, M.; Di Blasio, B.; Pedone, C. J Peptide Sci 1996, 2, 14–27.
24. Toniolo, C.; Crisma, M.; Formaggio, F.; Benedetti, E.; Santini, R.; Iacovino, M.; Saviano, M.; Di Blasio, B.; Pedone, C.; Kamphuis, J. Biopolymers (Peptide Sci) 1996, 40, 519–522.
25. Benedetti, E.; DiBlasio, B.; Iacovino, R.; Menchise, V.; Saviano, M.; Pedone, C.; Bonora, G.; M.; Ettorre, A.; Graci, L.; Formaggio, F.; Crisma, M.; Valle, G.; Toniolo, C. J Chem Soc Perkin Trans II 1997, 2023–2032.
26. Prasad, S.; Rao, R. B.; Balaram, P. Biopolymers 1995, 35, 11–20.
27. Benedetti, E.; Toniolo, C.; Hardy, P. M.; Barone, V.; Bavoso, A.; Di Blasio, B.; Grimaldi, P.; Lelj, F.; Pavone, V.; Pedone, C.; Bonora, G. M.; Lingham, I. J Am Chem Soc 1984, 106, 8146–8152.
28. Bonora, G. M.; Toniolo, C.; Di Blasio, B.; Pavone, V.; Pedone, C.; Benedetti, E.; Lingham, I.; Hardy, P. M. J Am Chem Soc 1984, 106, 8152–8156.
29. Dentino, A. R.; Pavone, V.; Raj, P. A.; Bhandary, K. K.; Wilson, M. E.; Levine, M. J. J Biol Chem 1991, 266, 18460–18468.
30. Di Blasio, B.; Pavone, V.; Isernia, C.; Pedone, C.; Benedetti, E.; Toniolo, C.; Hardy, P. M.; Lingham, I. N. J Chem Soc Perkin Trans II 1992, 523–526.
31. Prasad, S.; Mitra, S.; Subramanian, E.; Velumurugan, D.; Rao, R. B.; Balaram, P. Biochem Biophys Res Commun 1994, 198, 424–430.
32. Karle, I. L.; Rao, R. B.; Prasad, S.; Kaul, R.; Balaram, P. J Am Chem Soc 1994, 116, 10355–10361.
33. Benedetti, E.; Barone, V.; Bavoso, A.; Di Blasio, B.; Lelj, F.; Pavone, V.; Pedone, C.; Bonora, G. M.; Toniolo, C.; Leplawy, M. T.; Kaczmarek, K.; Redlinski, A. Biopolymers 1988, 27, 357–371.
34. Ragothama, S.; Chadda, M.; Balaram, P. J Phys Chem 1996, 100, 19666–19671.
35. Uma, K. (1990) Ph.D. thesis, Indian Institute of Science, Bangalore (Thesis Abstract, J Ind Inst Sci 1991, 71, 395–398).
36. Sheldrick, G. M. SHELXTL PLUS, Release 4.2 for Bruker R3m/V. Crystal Research System. Bruker Analytical X-Ray Instruments, Madison, WI, 1992.
37. Karle, I. L.; Flippen-Anderson, J.;L.; Uma, K.; Balaram, P. J Peptide Sci 1996, 2, 106–116.
38. Nagaraj, R.; Shamala, N.; Balaram, P. J Am Chem Soc 1979, 101, 16–20.
39. Bardi, R.; Piazzesi, A. M.; Toniolo, C.; Sukumar, M.; Balaram, P. Biopolymers 1986, 25, 1635–1644.
40. Bardi, R.; Piazzesi, A. M.; Toniolo, C.; Sukumar, M.; Raj, P. A.; Balaram, P. Int J Peptide Protein Res 1985, 25, 628–639.
41. Sudha, T. S.; Vijayakumar, S.; Balaram, P. Int J Peptide Protein Res 1983, 22, 464–468.
42. Wuthrich, K. NMR of Proteins and Nucleic Acids; John Wiley & Sons: New York,1986.
43. Neuhaus, D.; Williamson, M. The Nuclear Overhauser Effect In Structural and Conformational Analysis; VCSH Publishers, 1989.
44. Vijayakumar, E. K. S.; Balaram, P. Tetrahedron 1983, 39, 2725–2731.
45. Vijayakumar, E. K. S.; Balaram, P. Biopolymers 1983, 22, 2133–2140.
46. IUPAC-IUB Commission on Biochemical Nomenclature. Biochemistry 1970, 9, 3471–3479.